Water temperature modeling in the Lower Ebro River (Spain): Heat fluxes, equilibrium temperature, and magnitude of alteration caused by reservoirs and thermal effluent

Jordi Prats,[1] Rafael Val,[2] Josep Dolz,[1] and Joan Armengol[3]

Received 4 January 2011; revised 24 March 2012; accepted 26 March 2012; published 16 May 2012.

[1] The lower Ebro River (Spain) is subject to the thermal and hydrological alterations caused by the system of reservoirs of Mequinenza, Riba-roja, and Flix and to the thermal effluent of the nuclear power plant of Ascó, located 5 km downstream from the three reservoirs. In this paper, a modeling approach is used to determine the equilibrium temperature and recuperation distance at the study reach for different seasons and hydrological years. The intensity of the alteration caused by the reservoirs and nuclear power plant effluent is studied in reference to the equilibrium temperature and discharge rate. Mean daily water temperature downstream from the reservoirs is higher than mean daily equilibrium temperature in the fall and is lower during the rest of the year. Changes in the heat fluxes induced by thermal alteration are also addressed, showing important variations in evaporation and conduction to the atmosphere.

Citation: Prats, J., R. Val, J. Dolz, and J. Armengol (2012), Water temperature modeling in the Lower Ebro River (Spain): Heat fluxes, equilibrium temperature, and magnitude of alteration caused by reservoirs and thermal effluent, *Water Resour. Res.*, *48*, W05523, doi:10.1029/2011WR010379.

1. Introduction

[2] Numerous works have demonstrated the importance of the longitudinal dimension when assessing the effect of thermal alterations. Anthropogenic disturbances, such as reservoirs, thermal effluents, or reductions in river flow, as well as certain natural perturbations, suppose a discontinuity in the longitudinal organization of the river [*Ward and Stanford*, 1983, 1995; *Sabater et al.*, 1989; *Stanford and Ward*, 2001]. Downstream from the alteration point, the river tends to recover its natural behavior, and the discontinuity distance and intensity of the alteration depends on the type of river, climate, and kind of alteration. Additionally, *Polehn and Kinsel* [1997], *Lowney* [2000], *Khangaonkar and Yang* [2008], and *Tang and Keen* [2009] demonstrated that disturbances that alter the daily temperature cycle can induce a gradually fading node and antinode pattern of daily temperature range. Consequently, it does not suffice to consider water temperature at one site or average temperatures along a given reach downstream from a reservoir; it is necessary to consider water temperature all along the reach. Also, the persistence of alterations for long distances makes it possible that some river reaches are subject to multiple thermal disturbances [*Arrúe and Alberto*, 1986; *Bonacci et al.*, 2008; *Prats et al.*, 2010]. The study of the combined effects of different sources of thermal perturbation, though, has received little attention.

[3] However, many studies regarding thermal alterations in streams and rivers [*Lessard and Hayes*, 2003; *Steel and Lange*, 2007; *Zolezzi et al.*, 2010] and regulations, such as the EU Directive 2006/44/CE, do not consider the longitudinal effects of water temperature alterations, and they assess thermal alterations by comparing two points: one upstream and the other downstream from the alteration point [e.g., *Lessard and Hayes*, 2003; *Raddum et al.*, 2008; *Prats et al.*, 2010]. This approach does not consider the length of the river affected by a thermal discharge or the possible existence of complex spatial patterns of water temperature variability. Even those studies taking into account longitudinal variation in water temperature [*Webb and Walling*, 1993; *Preece and Jones*, 2002; *Frutiger*, 2004; *Prats et al.*, 2010] often do not cover the studied reach with enough spatial resolution to detect such patterns clearly. Additionally, this approach is biased unless steady state temperatures are equal at both upstream and downstream sites, given that meteorological variables and river hydraulics vary along the river with the natural consequence of varying steady state temperatures. Hence, while upstream-downstream comparisons seem adequate for point disturbances such as thermal effluents, in the case of lineal alterations, such as reservoirs (especially long ones) or forest clearances, the results may not be accurate due to different steady state temperatures at the upstream and downstream sites. In order to obtain a more accurate assessment of the effect of such types of alteration, not only the differences of water temperatures at both sites should be considered, but also the differences between their respective steady state temperatures. Besides, the alternative of comparing present conditions with those previous to the alteration

[1]Department of Hydraulic, Maritime and Environmental Engineering, Technical University of Catalonia, Barcelona, Spain.
[2]PUMAGUA, Universidad Nacional Autónoma de México, Ciudad Universitaria, Mexico.
[3]Department of Ecology, Faculty of Biology, University of Barcelona, Barcelona, Spain.

0043-1397/12/2011WR010379

[*Hamblin and McAdam*, 2003; *Steel and Lange*, 2007] is also problematic because of climate change. In many rivers, trends of increasing water temperature of between $\sim$0.01°C yr^{-1} and $\sim$0.1°C yr^{-1} have been observed and have been more intense in the last 25–30 yr [*Webb and Nobilis*, 1994; *Prats et al.*, 2007; *Bonacci et al.*, 2008; *World Wildlife Federation* (*WWF*), 2009].

[4] To assess the intensity of thermal alterations and avoid the climate change and geographical biases described above, it is necessary to compare altered water temperatures with a base reference that is specific to the place and time of measurement. The obvious choice would be *natural water temperature* at the measurement point, the water temperature that the river would have at that point if there were no anthropogenic alterations. However, natural water temperature is unknown and simulating it would be far too costly for most of applications. Instead, we use equilibrium temperature (defined as steady state temperature) as a base reference to assess water temperature alteration, an approach already followed by *Bogan et al.* [2003, 2004].

[5] Apart from the direct alterations caused by the altered temperature of water exiting the reservoirs and the nuclear power plant, indirect alterations on the thermal regime due to regulated river flow also occur. A reduction of river discharge increases water temperature variability due to reduced thermal inertia [*Gu et al.*, 1999; *Meier et al.*, 2003; *Prats et al.*, 2010]. Also, downstream from the confluence of a river affected by hydropeaking and an incoming flow with a different temperature (power plant effluent or tributary), hydropeaking can affect the river thermal cycle at subdaily scales and cause abrupt modifications in water temperature, known as thermopeaking, which are limited to the passage of the transient [*Frutiger*, 2004; *Zolezzi et al.*, 2010].

[6] In this paper, focus is placed on the combined effects of a system of reservoirs (Mequinensa, Riba-roja, and Flix) and the thermal effluent of the nuclear power plant of Ascó on the thermal dynamics of the lower Ebro River in eastern Spain. Downstream from the system of reservoirs, the Ebro River is also subject to regulation and important daily variations of discharge of 100 m^3 s^{-1} or more occur during most of the year, except in the summer [*Prats et al.*, 2009]. The present study is the continuation of a series of previous works [*Dolz et al.*, 1994; *Limnos*, 1997; *Val*, 2003; *Prats et al.*, 2010] carried out in the study area in response to the concern for the effects of thermal alterations due to the nuclear power plant on the river ecosystem. Ironically, research has shown that the system of reservoirs can produce thermal perturbations as important as those due to the nuclear power plant, and that the nuclear power plant warming effect in the summer tends to cancel the cooling effect of the system of reservoirs.

[7] This study tries to solve the drawbacks in previous research caused by comparisons of upstream-downstream conditions and of pre- and postalteration conditions, and by insufficient spatial resolution. First, we review the concept of equilibrium temperature and propose an alternative definition to the classical one. Then, we quantify the intensity of the alterations caused by the reservoirs and the nuclear power plant on a seasonal scale using two new indices: the difference of mean daily water temperature with respect to steady state temperature and the recuperation distance. Additionally, we use a process-based water temperature model, developed by the authors and calibrated with empirical river data, to analyze longitudinal thermal dynamics and the role of regulated river flow and hydropeaking on thermal dynamics.

2. Calculation of the Intensity of the Alterations Based on Equilibrium Temperature

[8] The concept of equilibrium temperature has been used for more than 40 yr, being originally defined as "the water surface temperature at which the net heat exchange across the water surface would be zero" [*Edinger et al.*, 1968], which we refer to as *surface equilibrium temperature*. A better definition for *equilibrium temperature* in rivers is "the temperature at which the net heat exchange would be zero." In fact, when using the surface equilibrium temperature as equilibrium temperature, it is assumed explicitly [e.g., *Caissie et al.*, 2005] or implicitly that other heat exchanges do not occur, or are negligible. In fully mixed rivers, this assumption has often been used [*Edinger et al.*, 1974; *Mohseni and Stefan*, 1999; *Caissie et al.* 2005], while others have used the difference between predicted surface equilibrium temperature and observed water temperatures to estimate additional heat exchanges [*Bogan et al.*, 2003, 2004]. Equilibrium temperature is usually calculated from mean daily values of meteorological variables [*Mohseni and Stefan*, 1999] as the temperature T_e that shows,

$$\sum_{n\_days} H_T(t, T_e) = 0, \tag{1}$$

where H_T (W m^{-2}) is net heat flux and t (s) is time. Equation (1) can be solved analytically [*Edinger et al.*, 1968; *Caissie et al.*, 2005] or numerically [*Bogan et al.*, 2003, 2004].

[9] On the other hand, other authors [*Gu et al.*, 1999] use an alternative definition of equilibrium temperature as "the temperature that the river would reach if all weather conditions were constant in time." This temperature actually represents the *far-field water temperature* [*Khangaonkar and Yang*, 2008] or *steady state temperature*. For a sinusoidal equilibrium temperature, mean daily steady state temperature equals mean daily equilibrium temperature [*Khangaonkar and Yang*, 2008]. Also, steady state temperature and equilibrium temperature coincide twice a day, the first being driven toward the second by heat exchange processes [*Edinger et al.*, 1968]. Consequently, steady state temperature has a lower temperature range and is delayed with respect to equilibrium temperature. The evolution of water temperature along a reach and how it tends to a steady state can be modeled by using the advection-diffusion equation. The widely used expression proposed by *Edinger et al.* [1974] is,

$$\frac{\partial T}{\partial t} + u\frac{\partial T}{\partial x} = \frac{\partial}{\partial x}\left(D\frac{\partial T}{\partial x}\right) + \frac{H}{\rho_w C_w d}(T_{st} - T). \tag{2}$$

T (°C) is water temperature, where T_{st} (°C) is steady state temperature, x (m) is the distance downstream from a given point, u (m s^{-1}) is the water velocity, D (m^2 s^{-1}) is a dispersion

coefficient in the direction of the flow, H (W m^{-2} °C^{-1}) is an overall heat exchange coefficient, ρ_w (kg m^{-3}) is water density, C_w (J kg^{-1} K^{-1}) is specific heat of water, and d is mean river depth (m). For mean daily water temperature, a solution to equation (2) is,

$$T_m = T_{st,m} + (T_{0m} - T_{st,m})\exp(-kx/u), \quad (3)$$

where T_m (°C) is mean daily water temperature, $T_{st,m}$ (°C) is mean daily steady state temperature, T_{0m} (°C) is mean daily temperature at the upstream end of the reach, and k (s^{-1}) is [*Edinger et al.*, 1968, 1974]

$$k = H/(\rho_w C_w d). \quad (4)$$

In this paper we compare the calculated equilibrium temperature (T_e) and steady state temperature ($T_{st,m}$) to show that they are not exactly equivalent and cannot be used on equal grounds. To assess water temperature alterations at a given point, we used $T_{0m} - T_{st,m}$, the difference between mean daily water temperature at that point and the mean daily steady state temperature, and recuperation distance X_{st}. If these variables are to be used as indicators of the intensity of a particular alteration, it is necessary that water temperature be in equilibrium before the alteration. Otherwise, or if we cannot ensure whether water temperature is in equilibrium before the alteration, $T_{0m} - T_{st,m}$ and X_{st} will still be useful as indicators of the intensity of alterations at the study location, including the combined effects of the different alterations upstream from that point. Mean daily steady state temperature $T_{st,m}$ and recuperation distance X_{st} were defined as the mean daily water temperature that the river would reach and the distance necessary for it to recuperate, if the river characteristics (morphological, hydraulic, etc.) and thermal behavior remained stable downstream. The recuperation distance X_{st} was estimated as the distance that makes the difference between $T_{st,m}$ and mean daily water temperature <0.5°C, obtained from

$$|T_m - T_{st,m}| \leq 0.5°\mathrm{C} \quad (5)$$

in equation (3). Hence,

$$X_{st} = \frac{u}{k}\ln|2(T_{0m} - T_{st,m})| = \frac{\rho_w C_w Q}{HW}\ln|2(T_{0m} - T_{st,m})|, \quad (6)$$

where A (m^2) is a cross-sectional area perpendicular to the flow and $Q = Wdu$ (m^3 s^{-1}) is the river discharge. If $|T_{0m} - T_{st,m}|$ was already <0.5°C, then X_{st} was considered to be zero. Although other spatial measures of alteration have been previously used, such as flow distance for half-life of excess temperature [*Edinger et al.*, 1974] or adjustment scale length [*Wåhlin and Johnson*, 2009], we believe the sense of X_{st} can be more easily grasped by nonexperts and be more useful for management decisions.

[10] Both $T_{0m} - T_{st,m}$ and X_{st} were used as indicators to estimate the intensity of the alterations produced by the nuclear power plant of Ascó and by the system of reservoirs of Mequinensa, Riba-roja, and Flix as follows: First, the water temperature model described in this paper was used to simulate water temperature behavior along theoretical 1000-km length reaches with the same characteristics as the Ebro River reaches Flix-Ascó (to study the effect of reservoirs) and Pas de l'Ase-Miravet (to study the effect of a nuclear power plant). Upstream boundary conditions for each reach were fixed as the water temperatures measured at the stations of Flix and Pas de l'Ase, respectively. To study the seasonal dependency of steady state temperature, meteorological data was divided into 3-month sets. The mean characteristics at the diel scale of each seasonal meteorological data set were extracted to obtain the typical day for each season and year and were fed into the model. Mean daily steady state temperature was estimated by fitting equation (3) to the mean daily-simulated water temperature. Equilibrium temperature was calculated numerically using the same data sets and equation (1). Eight runs were made in all for each hydrological year (two stations multiplied by four seasons).

3. Field Data

[11] A water temperature-monitoring program took place in the lower Ebro River in the period of 1997–2010 to study the alterations caused by a system of three reservoirs (Mequinensa, Riba-roja, and Flix) and a nuclear power plant (N. P. P. Ascó) downstream from their respective locations (Figure 1). Previous results [*Prats et al.*, 2010] showed that the nuclear plant effluent increased water temperature by 3°C on average all year-round, and that the system of reservoirs produced a warming effect in the fall-winter and a cooling effect in the spring-summer. Other effects due to the reservoirs were a decrease in the annual and daily water temperature ranges, and a delay of the annual maxima and minima.

[12] Four measuring stations were used for this study. A measuring station was located just downstream from the system of reservoirs at Flix. Two monitoring points were used to analyze the effect of the nuclear power plant. The first station (Ascó) was installed at the nuclear power plant intake, 5.3 km downstream from Flix. The next one (Pas de l'Ase) was installed 6.5 km downstream from the nuclear power plant. Another station (Miravet) was set 21.5 km downstream from the nuclear power plant. The reach Flix–Ascó was affected only by the thermal effect due to the system of reservoirs, whereas the reach Pas de l'Ase–Miravet was affected by both the system of reservoirs and the nuclear plant. The comparison between these two reaches allowed us to distinguish between the alteration effects caused by the system of reservoirs from those caused by the nuclear power plant. In the reach Ascó–Pas de l'Ase, the plume of the nuclear plant thermal effluent slowly mixed with the river water; by Pas de l'Ase, water temperature was laterally and vertically homogeneous. Since the distance between Ascó and Pas de l'Ase is 6.5 km and it takes the water ~2 h to travel from Ascó to Pas de l'Ase, for an accurate assessment of the effect of the nuclear power plant at the timescale of interest (10 min) the comparison of water temperatures at Ascó and Pas de l'Ase did not suffice. A modeling approach was used instead by comparing water temperature measured at Pas de l'Ase with simulated water temperature assuming no thermal effluent existed (see below). There were no measurements available

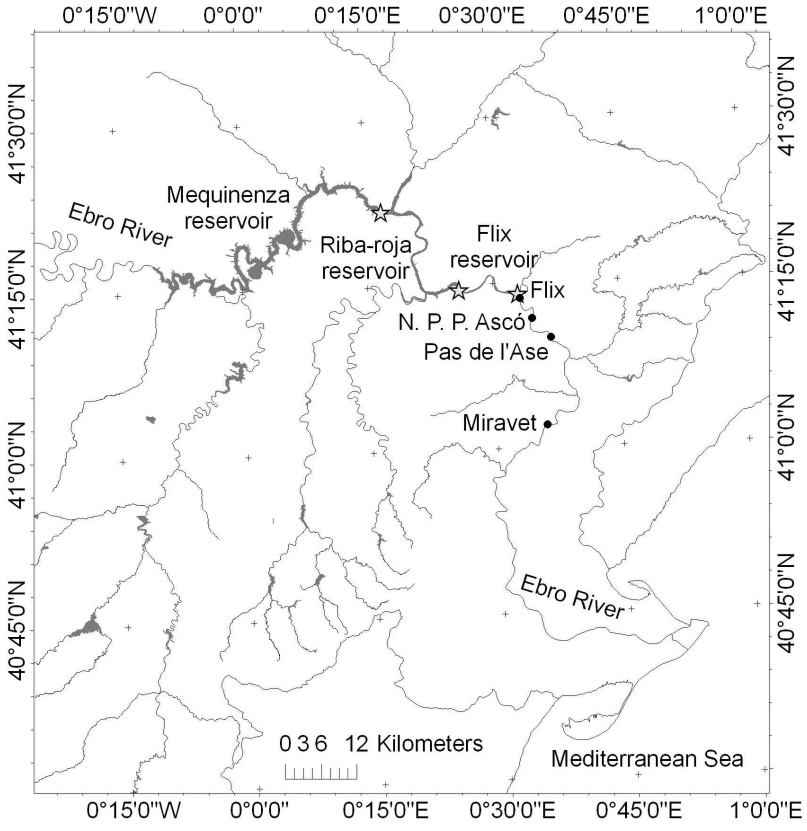

Figure 1. Study area. Reservoirs are shaded in gray; dams of Mequinenza, Riba-roja, and Flix are indicated with stars; and measuring stations are indicated with black dots.

upstream of the system of reservoirs in the study period. Water temperature, water levels, and meteorological data were measured every minute and the average was recorded every 10 min.

[13] Water temperature was measured by the riverside as an approximation to mean water temperature across the river. Lateral homogeneity of water temperature was checked by measuring several transections at Flix and Pas de l'Ase. Maximum lateral and vertical differences found were 0.1°C. Two or three probes were used to measure water temperature at each site as a control for measurement errors, sensor failures, calibration drifts, etc. The water temperature probes accuracy was ± 0.1°C according to the manufacturer, which was further improved to ± 0.04°C by measuring water temperature each minute and saving the 10-min average. Further errors were due to the data logger. As a result, sensor interchangeability (the difference in measurement between different sensors) was 0.1°C–0.2°C. When differences between sensors were >0.2°C, the probe(s) was (were) replaced. Overall accuracy resulting from all sources of error was 0.2°C–0.3°C.

[14] Flow records were provided by the Ebro Basin Water Authority (Confederación Hidrográfica del Ebro) and water levels were measured at Flix and Miravet. Using these data, stage-discharge relations and hydraulic parameters were derived. The analysis of stage-discharge relations in the years 2000–2006 showed variations of the river's hydraulic behavior attributable to macrophyte growth [*Prats et al.*, 2009]. The presence of macrophytes in a river can alter its hydraulic characteristics: it causes an increase in water levels, a decrease in water velocity, and it may produce vertical and spatial differences in water velocity [*Wilcock et al.*, 1999; *Champion and Tanner*, 2000; *de Doncker et al.*, 2009]. Consequently, the study periods were chosen so that the river hydraulics and its thermal behavior were not altered by the presence of macrophytes. A macrophyte-free stage-discharge relation with error bounds was defined using data for January–October 2001. Periods when daily stage-discharge measurements lay consistently outside the error bounds were filtered out as macrophyte affected [*Prats et al.*, 2009]. This filtering resulted in the selection of the hydrologic years 2000/2001, 2001/2002, and 2003/2004 (Figure 2), excepting the August 2001, November 2003, and July and August 2004 data, which were discarded from the analysis due to macrophyte-affected intervals. The hydrological years 2000/2001 and 2003/2004, with mean annual discharges of 401.5 $m^3 s^{-1}$ and 444.2 $m^3 s^{-1}$, respectively, can be considered relatively wet years. Peak discharge floods of 1650 $m^3 s^{-1}$, 2384 $m^3 s^{-1}$, and 2490 $m^3 s^{-1}$ were registered in 2000/2001. In 2003/2004 there were no important floods, but discharge was high during most of the fall and all of the winter. Instead, 2001/2002 was a very dry hydrological year with a mean annual discharge of 129.2 $m^3 s^{-1}$. In addition, most of winter water temperatures measured at Flix in 2002 were also discarded due to a lack of representation.

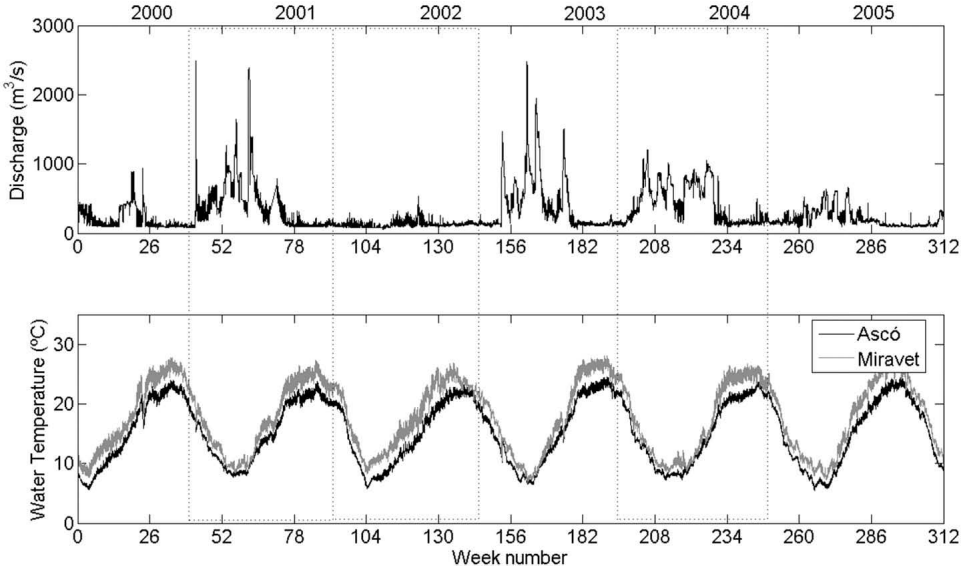

Figure 2. Discharge and water temperature (10-min data) in the study area in the years 2000–2005. Study periods are indicated.

4. Description of the Model

4.1. Governing Equations

[15] Assuming that each river section is homogeneous, that is, well mixed laterally and vertically, the water temperature along the longitudinal dimension of the river can be simulated by using the one-dimensional advection-diffusion equation,

$$\frac{\partial T}{\partial t} + u\frac{\partial T}{\partial x} = \frac{\partial}{\partial x}\left(D\frac{\partial T}{\partial x}\right) + \frac{(H_A W + H_b W_b)}{A\rho_w C_w}, \tag{7}$$

where H_A (W m^{-2}) is heat flux between the water and the atmosphere, H_b (W m^{-2}) is heat flux through the riverbed, W (m) is the river width, and W_b (m) is the wetted perimeter. *Pujol and Sánchez-Cabeza* [2000] found $D \approx 400$ m^2 s^{-1} for $u = 0.9$ m s^{-1} in the study area (from the nuclear power plant to Miravet). Since the distance from Pas de l'Ase to Miravet is $L = 21.5$ km, the Péclet number is $Pe = D/uL = 0.02 << 1$, meaning that advection dominates and diffusion is not important in the study reach. Equation (7) can then be simplified to obtain the convection equation,

$$\frac{\partial T}{\partial t} + u\frac{\partial T}{\partial x} = q, \tag{8}$$

where q (°C s^{-1}) is equal to the source term

$$q = \frac{H_A W + H_b W_b + Q_{in}(T_{in} - T)}{A\rho_w C_w}, \tag{9}$$

where Q_{in} (m^3 s^{-1}) and T_{in} (°C) are incoming flow and water temperature of tributaries. In wide and shallow rivers, it may be assumed that $W = W_b$. Thus, taking $d = A/W$, and since there are no important tributaries in the study area, we can write:

$$q = \frac{(H_A + H_b)W}{A\rho_w C_w} = \frac{H_T}{d\rho_w C_w}, \tag{10}$$

where H_T (W m^{-2}) denotes net heat flux between the water and the environment (atmosphere and riverbed).

[16] The flow-routing method used was the Muskingum-Cunge method, which is an approximate solution of the diffusion equation by means of a three-point finite difference scheme [*Ponce*, 1989],

$$Q_{i+1}^{n+1} = C_1 Q_i^{n+1} + C_2 Q_i^n + C_3 Q_{i+1}^n, \tag{11}$$

where Q_i^n is discharge at time $n\Delta t$ and distance $i\Delta x$, and

$$C_1 = \frac{\Delta t - 2KX}{2K(1-X) + \Delta t}, \tag{12}$$

$$C_2 = \frac{\Delta t + 2KX}{2K(1-X) + \Delta t}, \tag{13}$$

$$C_3 = \frac{2K(1-X) - \Delta t}{2K(1-X) + \Delta t}, \tag{14}$$

where Δt is the time step and $K = \Delta x/c$ is the travel time to cross a distance Δx at the wave celerity c. The coefficient X is a weighting factor representing numerical diffusion and adjusted to match hydraulic diffusion [*Cunge*, 1969]. Both parameters K and X were calibrated using river discharge data in the study reach.

[17] The heat flux H_T is positive when the river gains heat and can be expressed as,

$$H_T = H_A + H_b, \tag{15}$$

with

$$H_A = H_{sn} + H_{an} + H_w + H_e + H_c, \tag{16}$$

where H_{sn} (W m^{-2}) is net solar radiation, H_{an} (W m^{-2}) is net atmospheric long-wave radiation, H_w (W m^{-2}) is long-wave radiation emitted by the water surface, H_e (W m^{-2}) is

evaporative heat flux, and H_c (W m^{-2}) is convective heat flux. H_{sn} was calculated using the method proposed by *Campbell and Aarup* [1989], H_{an} was calculated using one of the parameterizations obtained by *Aubinet* [1994], H_w was calculated using the usual gray body formula with emissivity $\varepsilon_w = 0.97$, H_e was calculated using *Sill*'s [1983] method, and H_c was calculated from H_e using the Bowen ratio [*Henderson-Sellers*, 1986]. In an early version of this study H_b was calculated and was found to always be in the range ± 5 W m^{-2} and considered negligible. In consequence, H_b was not used in the final analysis. Formulations, further details, and a discussion regarding heat flux calculations can be found in the supplementary material.[1]

4.2. Numerical Model

4.2.1. Description of Numerical Model

[18] A numerical model developed in the MATLAB environment was used to simulate hydrodynamics, water temperature, and heat fluxes longitudinally in selected reaches in the Ebro River. Discretization of the model was defined as $\Delta t = 600$ s for the time steps and $\Delta x \approx 1000$ m for the length steps (see Table 1), to allow sufficient detail in the calculations with a low computation effort. Two uncoupled modules were used to separately calculate the hydrodynamics and the water temperature. The hydrodynamic module uses the Muskingum-Cunge model for flow routing along the selected reaches. The thermal module solves equation (8) by using the method of characteristics.

[19] Water temperature simulations were made for three reaches: Flix-Ascó, Ascó-Pas de l'Ase, and Pas de l'Ase-Miravet. Upstream boundary conditions consisted of flow and water temperature at the upstream end of each reach. Flow was measured at Flix and routed down to Ascó, Pas de l'Ase, and Miravet. Water temperature at the upstream end of each reach was measured. The thermal effluent of the nuclear power plant was located about 100 m downstream from the upstream end of the reach Ascó-Pas de l'Ase. Unfortunately, thermal effluent discharge and temperature data were not publicly available. As a consequence, for this reach, simulated water temperature corresponds to expected water temperature if thermal discharge did not take place, and was used to estimate the nuclear power plant effect by the difference with respect to measured water temperature at the downstream end (Pas de l'Ase). Lateral boundary conditions for all of the reaches consisted of heat exchange calculated according to equations (15) and (16) and using meteorological data (air temperature, relative humidity, short-wave radiation, and wind speed). Since comparisons of meteorological data measured at Miravet with data from other riverine meteorological stations in the area provided by the Meteorological Service of Catalonia did not reveal important differences, meteorological forcing was applied uniformly to the entire model domain. The calculations were made in weekly periods.

4.2.2. Calibration and Validation

[20] The hydrodynamic parameters were assumed to be uniform over the simulation domain and were calibrated by using field data for the years 2000 and 2001. The parameters

Table 1. Discretization Used for Each of the Selected Reaches

Reach	Reach Length (m)	Δx (m)	Δt (s)
Flix-Ascó	5300	1060	600
Ascó-Pas de l'Ase	6500	1083	600
Pas de l'Ase-Miravet	21,500	1075	600

K and X of the Muskingum-Cunge method were calibrated for the full reach Flix-Miravet. Although a water velocity-discharge relation had already been derived by *Pujol and Sánchez-Cabeza* [1999, 2000], the results provided by the model often were out of phase with measured water temperatures if their velocities were used. It is probable that the expression presented in their work was no longer applicable due to dredging works done (after their measurements) in the river to make it navigable and that modified its hydraulic behavior. The water velocity-discharge relation was calibrated by minimizing the sum of quadratic errors in the reach Pas de l'Ase-Miravet and the calibrated expression was used for the entire modeling domain. The parameters of the thermal processes were not calibrated, as the model already provided sufficiently accurate results.

[21] The model was validated for the reaches Flix-Ascó and Pas de l'Ase-Miravet for the three hydraulic years 2000/2001, 2001/2002, and 2003/2004. Conservation of mass and heat in the simulations were checked. Model performance was assessed with average error (AE), mean absolute error (MAE), modeling efficiency (ME), and benchmark efficiency (BE) [*Janssen and Heuberger*, 1995; *Willmott and Matsuura*, 2005; *Schaefli and Gupta*, 2007],

$$\mathrm{AE} = \frac{\sum (P_i - O_i)}{n}, \tag{17}$$

$$\mathrm{MAE} = \frac{\sum |P_i - O_i|}{n}, \tag{18}$$

$$\mathrm{ME} = 1 - \frac{\sum (P_i - O_i)^2}{\sum (O_i - \overline{O})^2}, \tag{19}$$

$$\mathrm{BE} = 1 - \frac{\sum (P_i - O_i)^2}{\sum (O_i - U_i)^2,} \tag{20}$$

where P_i and O_i are predicted and observed values at the downstream end of the reach, U_i are measured values at the upstream end of the reach, n is the number of observations, and $\overline{O}$ is the mean of the observed values. The modeling efficiency is a measure of the relative improvement of the model used over a benchmark situation $\overline{O}$ [*Janssen and Heuberger*, 1995]. However, to assess more accurately the usefulness of a model, it may be advisable to define an alternative reference situation, and thus obtain the benchmark efficiency [*Schaefli and Gupta*, 2007]. The baseline used herein is the upstream measured values, U_i.

5. Results

5.1. Model Performance

[22] Model performance results are presented in Figure 3 and Table 2. Figure 3 shows the cumulative distribution

[1] Auxiliary materials are available in the HTML. doi:10.1029/2011WR010379.

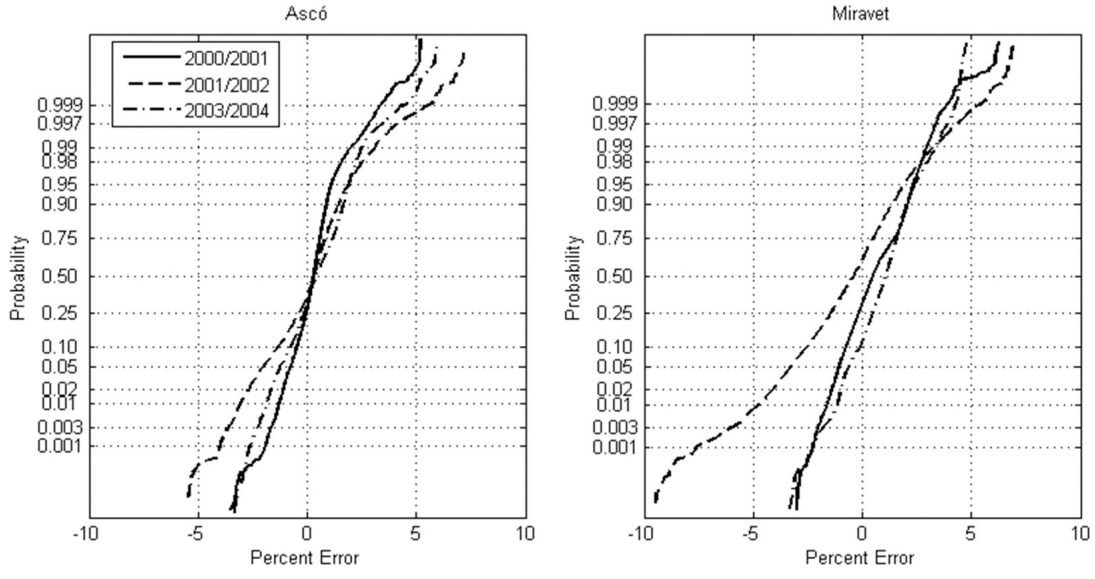

Figure 3. Cumulative probability distribution of the percent difference between measured and estimated water temperatures at Ascó and Miravet every 10 min.

function of the percent error for the different stations and hydrologic years. For each year, the error is within 5% more than 99% of the time. Somewhat higher errors were found for the estimations at Miravet for hydrologic year 2001/2002. Summary performance values are given in Table 2. In the first two hydrologic years, the average error is on the order of −0.06°C–0.16°C at Miravet, while at Ascó there is a slight overestimation of 0.03°C–0.04°C. The mean average error is greater at Miravet (with a value of ∼0.2°C), than at Ascó (∼0.1°C). This simulation error is on the same order as the measuring error. The modeling efficiency is very high in all of the cases. It is nearly equal to one: 0.997 at Ascó and 0.983 at Miravet. Considering the improvement with respect to initial upstream water temperatures, given by the defined benchmark efficiency, good BE values of 0.79–0.91 are still obtained at Miravet, and are poorer at Ascó (0.57–0.71). According to these BE values, it would seem that the model does not provide a significant enhancement in the simulation of water temperatures for the stretch Flix–Ascó in contrast to high ME values. Such high ME values for the stretch Flix–Ascó occur because the influence of upstream water temperature can still be sensed at the end of the reach. From Flix to Ascó, water temperature usually changes just by a few tenths of degree, which explains the limited improvement of using the model with respect to the initial upstream temperatures, and the lower BE values with respect to Miravet's BE values. Given the small variation in water temperature in the reach Flix–Ascó, it is difficult to determine whether the model is sensitive to this reach or not, the reach is too short. However, since the model predictions are accurate for the reach Pas de l'Ase–Miravet and both reaches have similar meteorology and river characteristics (morphological, hydraulic, etc.), we believe the predictions provided for the reach Flix–Ascó can be accepted confidently.

[23] Figure 4 shows the upstream and downstream measured water temperatures at the reaches Flix–Ascó and Pas de l'Ase–Miravet, as well as the simulated water temperature at the downstream end of the reaches and discharge at Flix, during five selected weeks covering different times of the year and hydrological situations. In the 5 km distance between the Flix and Ascó measurement stations, water temperature change is nearly negligible. Conversely, in the reach Pas de l'Ase-Miravet, water temperature change is insignificant when discharge is high (weeks 72 and 215 in Figure 4), yet is notable when discharge is low (weeks 86, 96, and 215). In each case, the model provides very good estimations and follows well the daily water temperature variations, indicating that the model is capable of simulating water temperature in the study reach at different times of the year and hydrological situations.

5.2. Nuclear Power Plant Effect

[24] The effect of the Ascó nuclear power plant on water temperature was estimated as the difference between water temperature measurements at Pas de l'Ase and water temperature estimated at the same point with no nuclear thermal effluent (Figure 5). For these calculations the reach

Table 2. Model Performance at the End of the River Reaches Flix-Ascó and Pas de l'Ase-Miravet

	T at Ascó				*T* at Miravet			
Hydrological Year	AE (°C)	MAE (°C)	ME	BE	AE (°C)	MAE (°C)	ME	BE
2000/2001	0.04	0.08	0.999	0.715	0.08	0.16	0.999	0.904
2001/2002	0.03	0.13	0.998	0.574	−0.07	0.19	0.997	0.898
2003/2004	0.03	0.11	0.999	0.580	0.16	0.18	0.999	0.790

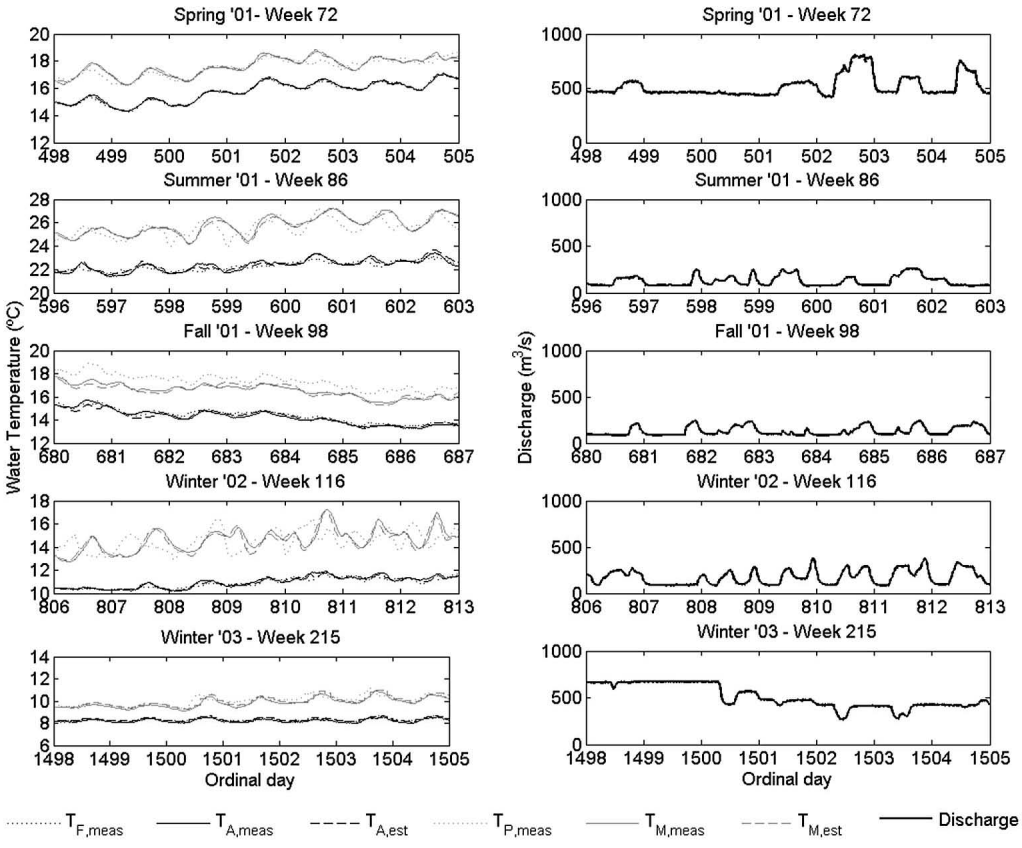

Figure 4. Water temperatures (right column) and discharge at Flix (left column) every 10 min during five selected weeks: measured water temperatures at Flix ($T_{F,\mathrm{meas}}$), Ascó ($T_{A,\mathrm{meas}}$), Pas de l'Ase ($T_{P,\mathrm{meas}}$), and Miravet ($T_{M,\mathrm{meas}}$); estimated water temperatures at Ascó ($T_{A,\mathrm{est}}$) and Miravet ($T_{M,\mathrm{est}}$).

considered was Ascó-Pas de l'Ase, and upstream boundary temperature was considered to be the water temperatures measured at Ascó. As shown in Figure 5, water temperature alteration is highly irregular, with its magnitude depending on discharge. As hydropeaking occurs in the studied river reach, the important and rapid variations in discharge induce important and rapid variations in water temperature. Increased water temperature variability is observed, and water temperature oscillations can lose their daily periodicity. The relation between water temperature and discharge is not simple, especially for lower discharges, because the amount of heat released to the water is not constant [*Prats et al.*, 2010]. The function of free and forced convection towers is variable depending on environmental conditions, and is managed so as to comply with legal limitations of water temperature increases.

5.3. Heat Exchange Processes

[25] Figure 6 shows mean weekly values of the different heat fluxes calculated by the model. The gaps in the series are caused by macrophyte affecting the river or sensor malfunctioning. The increase in downstream water temperature from the Ascó nuclear power plant accounts for higher heat losses at the reach Pas de l'Ase-Miravet than at the reach Flix–Ascó and the different behavior regarding H_c and H_e. Conduction is negative during the first half of the hydrological year at Flix (down to -50 W m^{-2}), and is positive during the second half (up to 50 W m^{-2}), whereas it is negative during the first half of the year at Pas de l'Ase (down to -50 W m^{-2}), and approximately neutral during the rest of the year.

5.4. Steady State Temperature and Equilibrium Temperature

[26] Table 3 shows the results of adjusting equation (3) to simulated water temperatures in theoretical 1000-km long reaches with seasonal average initial water temperatures and meteorological parameters at Flix and at Pas de l'Ase, as well as equilibrium temperatures (equal for both reaches since the meteorological data used is the same). Mean daily steady state temperatures estimated for both sites were almost the same with a maximum difference of 0.3°C in the fall of 2000. $T_{st,m}$ was highest for a typical day in summer, with values of 26°C–28°C, and lowest in the winter, at ~10°C–12°C. Additionally, $T_{st,m}$ was lower in the fall (with values of 11°C–13°C) than on an average spring day (~22°C). T_e had the same annual behavior as $T_{st,m}$, but were ~1°C higher. Seasonal mean typical day water temperatures and steady state temperatures were very similar from one year to the other. T_{0m} at Pas de l'Ase was higher than at Flix, due to the alteration effect of the nuclear power plant (estimated as ΔT_{0m}), which oscillated between 1.0°C and 3.9°C. The nuclear power plant alteration was negatively correlated with discharge (Pearson correlation coefficient of -0.768 significant at the 0.01 level). The higher the discharge, the less significant is the water

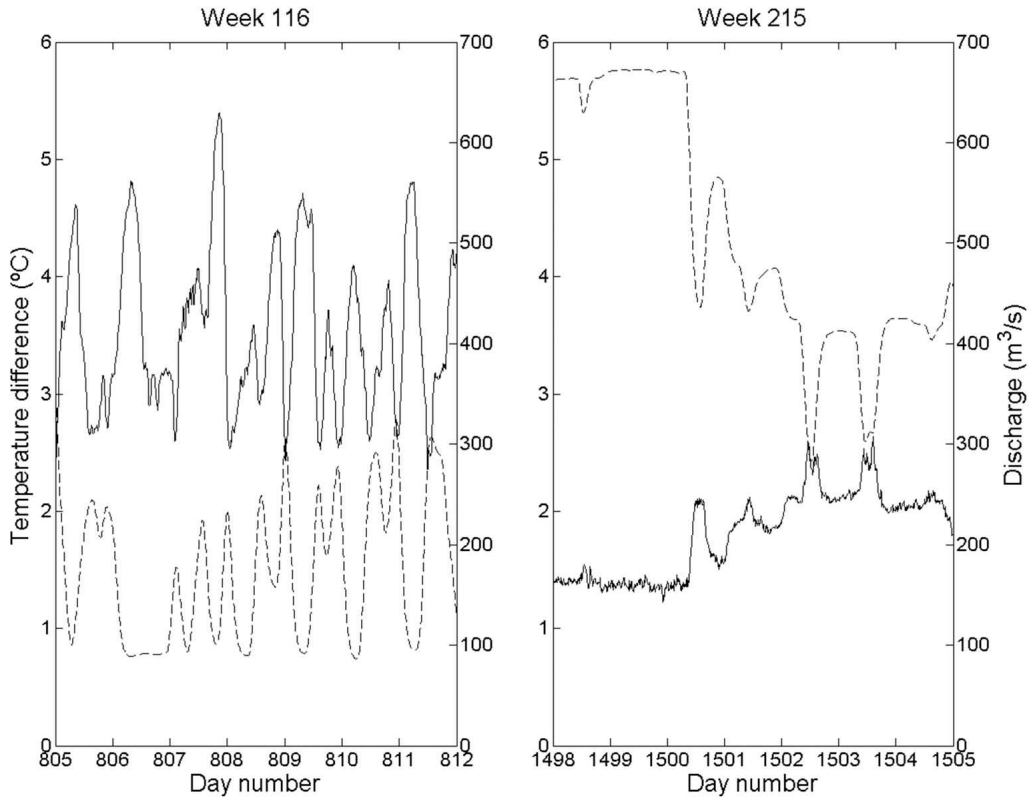

Figure 5. Difference between 10-min water temperatures measured at Pas de l'Ase and estimated without nuclear power plant effect and discharge.

temperature alteration due to increased thermal inertia. The heat exchange coefficient k varied between 0.87×10^{-6} s^{-1} and 3.17×10^{-6} s^{-1} at Flix, and was slightly higher at Pas de l'Ase (ranging between 0.97×10^{-6} s^{-1} and 3.58×10^{-6} s^{-1}). Thus, the time constant k^{-1} range was 1.8–6.6 h at Flix, and 2.0–7.4 h at Pas de l'Ase. Heat exchange was most intense in the summer and lowest in the winter.

[27] Mean daily steady state temperatures were higher than initial temperatures T_{0m} in the fall at both stations: 1°C–2.5°C higher at Flix, and 3°C–5.5°C higher at Pas de

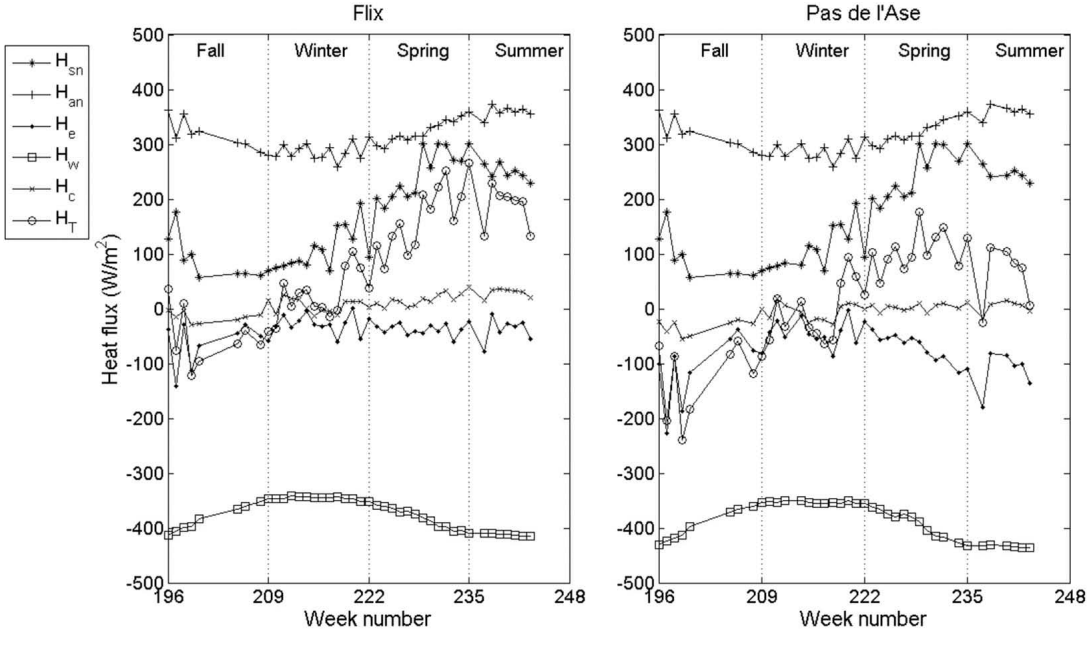

Figure 6. Mean weekly heat exchange at Flix and Pas de l'Ase during hydrological year 2003/2004.

Table 3. Mean Daily Initial and Equilibrium Temperatures, Time Constant, and Recuperation Distance for Seasonal Typical Days in the Hydrological Years 2000/2001, 2001/2002, 2003/2004

				Flix					Pas de l'Ase					Pas de l'Ase–Flix	
Period	Q ($m^3 s^{-1}$)	U ($m s^{-1}$)	T_e (°C)	$T_{st,m}$ (°C)	T_{0m} (°C)	K ($\times 10^{-6} s^{-1}$)	$T_{0m} - T_{st,m}$ (°C)	X_{st} (km)	$T_{st,m}$ (°C)	T_{0m} (°C)	K ($\times 10^{-6} s^{-1}$)	$T_{0m} - T_{st,m}$ (°C)	X_{st} (km)	ΔT_{0m} (°C)	ΔX_{st} (km)
							2000/2001								
Fall	372	0.99	14.0	12.7	14.4	1.34	1.7	899	13.0	16.0	1.70	3.0	1043	1.6	144
Winter	743	1.28	13.1	12.0	8.6	0.87	−3.4	2804	11.8	10.3	0.97	−1.6	1499	1.6	−1304
Spring	294	0.91	23.2	22.4	16.2	2.21	−6.2	1033	22.3	18.0	2.34	−4.3	835	1.8	−198
Summer	111	0.63	27.2	26.2	21.1	3.17	−5.1	463	26.2	24.3	3.58	−1.9	235	3.2	−228
							2001/2002								
Fall	126	0.66	12.5	11.2	13.7	1.84	2.5	580	11.3	16.8	2.14	5.5	738	3.1	158
Winter	109	0.63	13.0	–	–	–	–	–	11.7	11.7	–	0.0	0	–	–
Spring	200	0.79	22.3	21.7	14.7	2.35	−7.0	884	21.6	18.7	2.69	−2.9	513	3.9	−368
Summer	244	0.85	27.6	26.4	20.4	2.65	−6.0	794	26.2	23.9	3.06	−2.3	426	3.5	−368
							2003/2004								
Fall	418	1.03	14.0	12.8	13.9	1.32	1.1	601	13.0	16.2	1.56	3.2	1220	2.3	619
Winter	654	1.22	12.0	10.6	8.6	1.01	−2.0	1684	10.5	10.1	1.15	−0.4	0	1.5	−1684
Spring	543	1.14	22.3	22.2	15.6	1.69	−6.6	1740	22.0	16.6	1.80	−5.4	1501	1.0	−239
Summer	233	0.83	28.5	27.7	21.4	2.66	−6.3	793	27.6	25.1	3.08	−2.4	426	3.8	−367

l'Ase, yet they were lower than T_{0m} during the rest of the year. Maximum differences between $T_{st,m}$ and T_{0m} were found in the summer, when T_{0m} was 6°C–7°C lower than $T_{st,m}$ at Flix, and 3°C–5°C lower than $T_{st,m}$ at Pas de l'Ase. Differences between $T_{st,m}$ and T_{0m} in the winter at Pas de l'Ase are minor, especially in the years 2001/2002 and 2003/2004, when water was near thermal equilibrium.

[28] Figures 7a, 8a, and 9a show the simulated water temperatures along 1000-km long reaches with seasonal average initial water temperatures and meteorological parameters at Flix in the spring of 2001 (Figure 8), and at Pas de l'Ase in the fall of 2000 (Figure 7) and the winter of 2002 (Figure 9). Each figure represents a different situation regarding the relationship between T_{0m} and T_{st}: $T_{0m} > T_{st,m}$ is presented in Figure 7, $T_{0m} < T_{st,m}$ in Figure 8, and $T_{0m} \approx T_{st,m}$ in Figure 9. The initial and final temperatures and the initial discharge in the course of the day are shown in Figures 7b, 8b, and 9b. As water travels downstream, the mean daily water temperature approaches mean daily steady state temperature and a steady state is eventually attained, at which the water temperature cycle remains the same as water flows downstream. Since the reservoirs alter the daily water temperature cycle, daily water temperature range and timing of the daily maxima and minima normally do not coincide with those of the thermal steady state. In some cases, as in Figure 9, it is even possible that a mean daily water temperature is in equilibrium, while its daily variation is not. When the daily thermal cycle is not in a stationary situation, a pattern of nodes and antinodes of daily temperature range is created, disappearing as water approaches the thermal equilibrium situation. The velocity at which the water temperature approaches steady state depends on discharge and heat exchange. Figures 7c, 8c, and 9c present the heat fluxes at the upstream end of the reach, and Figures 7d, 8d, and 9d reflect the downstream end. The main differences between upstream and downstream end heat fluxes are found in heat conduction (H_c) and, primarily, in evaporation (H_e). When $T_{0m} > T_{st,m}$, water temperature diminishes downstream, and evaporative losses decrease and conduction increases. On the other hand, when $T_{0m} < T_{st,m}$, losses of latent and sensible heat become more important as water temperature increases downstream. Finally, small changes in emitted long-wave radiation caused by the water temperature variation are also observed.

[29] In the spring of 2001 (Figure 8), and also in other cases not shown, the daily water temperature range varied irregularly with distance. This irregular behavior was caused by the daily pattern of discharge with two peaks of discharge, one in the morning and the other at night. If the calculations were repeated for a constant discharge, a clear pattern of nodes and antinodes of daily water temperature range was observed.

5.5. Recuperation Distance

[30] Recuperation distance in the Ebro River is of the order of 10^2 km–10^3 km, as shown in Table 3. For Flix, X_{st} takes values from ~450 to ~2800 km. For Pas de l'Ase, the increase in water temperature caused by the nuclear power plant effluent produces an increase in X_{st} in the fall and a reduction during the rest of the year, as shown by ΔX_{st}. X_{st} clearly depends on the alteration intensity

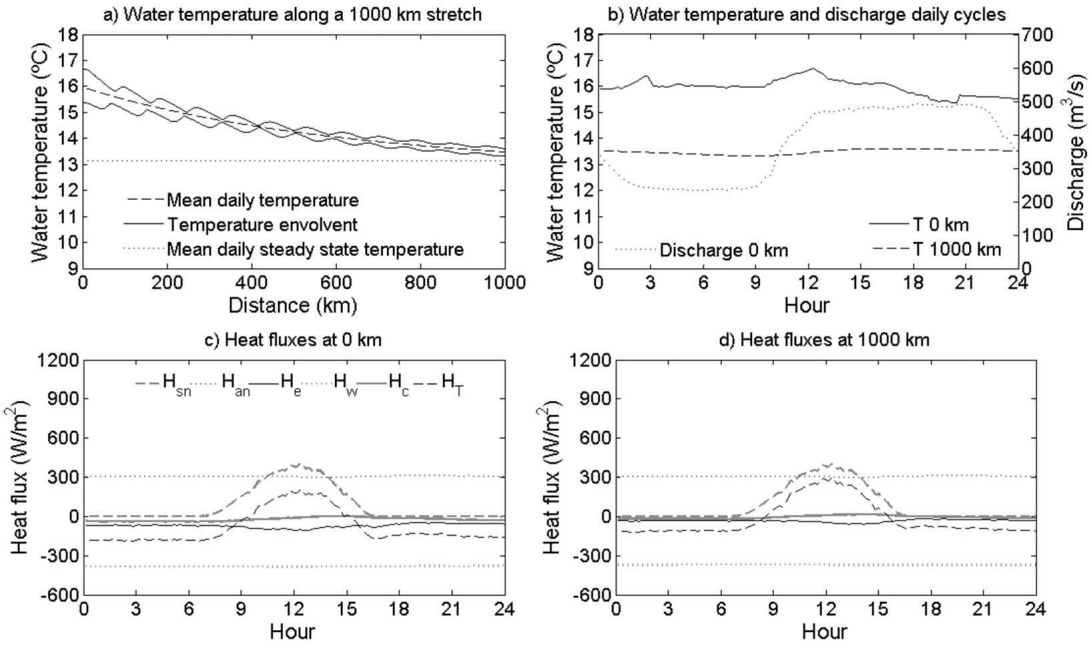

Figure 7. (a) Simulated water temperature along a theoretical 1000 km reach, (b) typical daily data at Pas de l'Ase during the fall of 2000 used in the calculation (0 km) and calculated water temperature at 1000 km, and heat fluxes at (c) the beginning and (d) the end of the reach.

$T_{0m} - T_{st,m}$, water velocity u, heat exchange coefficient k, river geometry, and discharge (see equation (6)). Figure 10 shows the variation of X_{st} as a function of $T_{0m} - T_{st,m}$, u, and k, for the range of values that can be found in the lower Ebro River. The value of $u = 1.0$ m s^{-1} appearing in the upper panel corresponds to a discharge of $\sim$400 m^3 s^{-1}, approximately the mean annual flow for the period 1953–2004. The value of $k = 2.0 \times 10^{-6}$ s^{-1} ($k^{-1} = 4.1$ h) appearing in the lower panel could be a typical spring value. Low values of X_{st} (<100 km) in the Ebro River are expected only for low thermal impacts (<1°C). Under most scenarios, though, X_{st} is at least 500 km, more than the distance to the sea.

[31] The multiple dependence of X_{st} on flow rate, water velocity, intensity of the alteration, and thermal processes explains why the river needs less distance to recover from

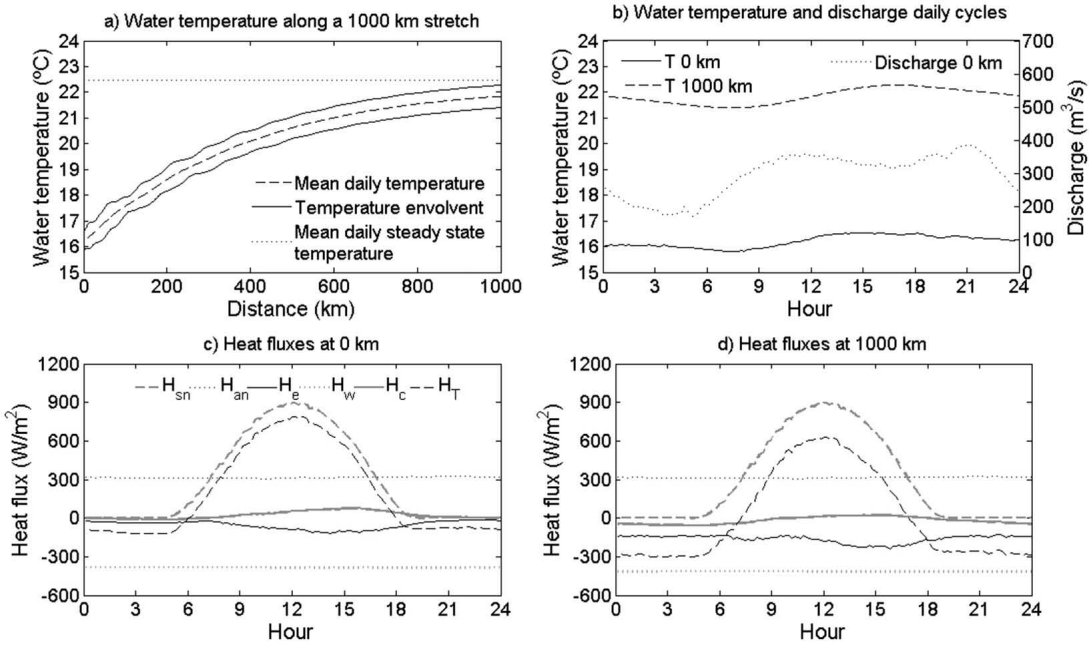

Figure 8. (a) Simulated water temperature along a theoretical 1000 km reach, (b) typical daily data at Flix during the spring of 2001 used in the calculation (0 km) and calculated water temperature at 1000 km, and heat fluxes at (c) the beginning and (d) the end of the reach.

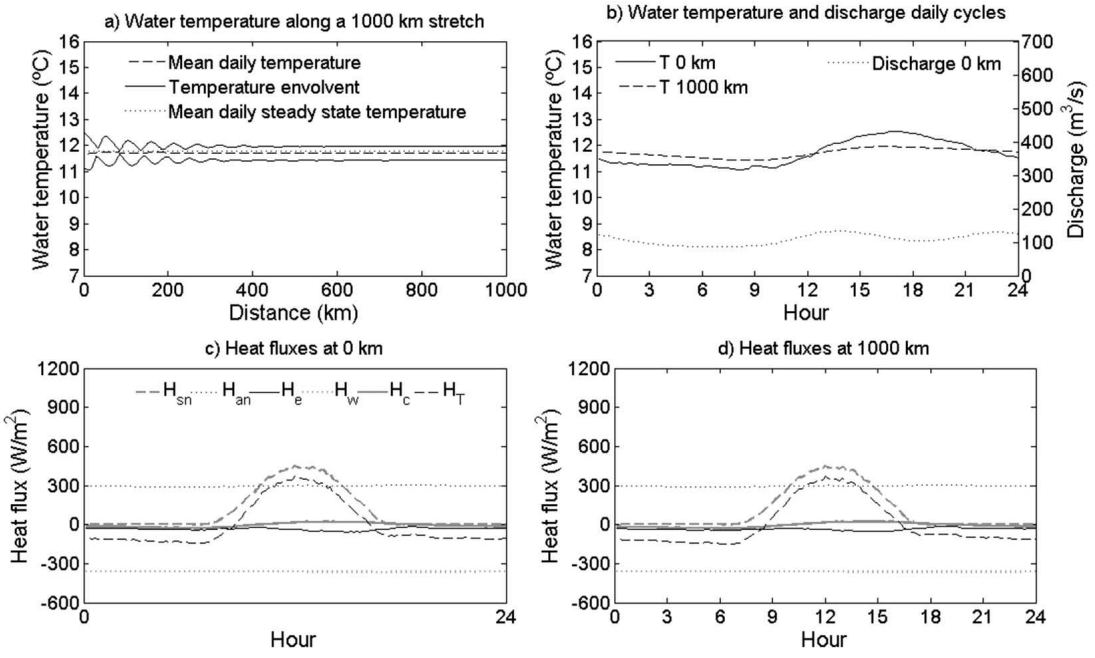

Figure 9. (a) Simulated water temperature along a theoretical 1000 km reach, (b) typical daily data at Pas de l'Ase during the winter of 2002 used in the calculation (0 km) and calculated water temperature at 1000 km, and heat fluxes at (c) the beginning and (d) the end of the reach.

an alteration of 7.0°C at Flix in the spring of 2002 than from an alteration of a magnitude of about half that in the wet winter of 2001. Although in the winter of 2001 T_{0m} is only 3.4°C lower than $T_{st,m}$, discharge is more than three times that observed in the spring of 2002, which implies a more significant thermal inertia. In the spring of 2002, k was more than 2.5 times higher than in the winter of 2001. In addition, at that time, water velocity was nearly doubled, resulting in a transport of the disturbance farther downstream, with the heat response being lower. Finally, river geometry can also influence X_{st}, since changes in W, d, and u can occur without Q being modified.

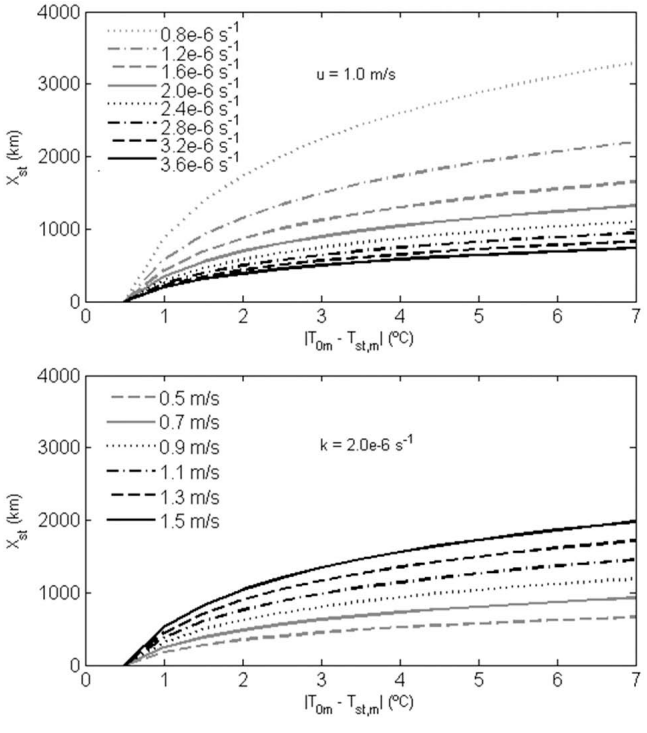

Figure 10. Dependence of recuperation distance X_{st} on heat exchange coefficient k (upper panel), and on water velocity u (lower panel).

6. Discussion

6.1. Heat Exchange

[32] *Webb and Zhang* [1997, 2004] found regulation effects on river heat fluxes in the River Haddeo, U.K., resulted in modifying long-wave radiation, increasing losses in the autumn and winter months, but having low values in the summer period. In the 1000-km long reach simulations for Flix data, similar seasonal differences are observed between upstream and downstream ends. Increased water temperatures in autumn and winter and reduced temperatures in spring and summer downstream from a reservoir cause H_w to increase in autumn and winter and to decrease in spring and summer. Additionally, H_w downstream from the nuclear plant of Ascó is higher than upstream due to increased water temperatures. However, in contrast with *Webb and Zhang*'s [1997, 2004] observations, in our study, the regulation had a more important effect on evaporation. The differences may be due to diverging environmental characteristics such as sheltering, windiness, air temperature, etc.

[33] Heat exchange processes that are functions of water temperature are evaporation, conduction with the atmosphere, emission of long-wave radiation, and conduction with the riverbed. A water temperature increase enhances losses of heat by conduction to the atmosphere and, most importantly, by evaporation, because of the increased

difference with respect to air temperature T_a. For example, at $T_a = 15°C$ and $T = 20°C$, an increase of 1°C in water temperature amplifies the losses of heat by evaporation by 24 W m^{-2} and by exchange of sensible heat by 14 W m^{-2}. Water temperature changes are not significant enough to induce important changes in emitted long-wave radiation: for water temperatures between 0°C and 35°C, a water temperature increase of 1°C causes an increase in emitted long-wave radiation of only ~4–6 W m^{-2}. Consequently, we may say that the main mechanism for a river to recover from a water temperature alteration is a modification in the exchange of latent and sensible heat, given that the other heat exchange processes remain more or less the same after the alteration. This means that a heated river will have difficulty losing excess heat if the atmospheric air is saturated with water, if it is sheltered (by trees or orographic features), if the wind speed is low, or the river morphology is not favorable to the loss of heat (e.g., narrow, deep sections).

6.2. Equilibrium Temperature and Water Temperature Alterations

[34] The simulations made with virtual 1000 km reaches show that, for the Ebro River, recuperation distances are of the order of 10^2 km–10^3 km. The calculated recuperation distance, though, is not the actual distance the river needs to recover from an alteration. Changes in meteorological conditions or river geometry downstream from the source of thermal alteration eventually modify the final distance for recuperation. In the Ebro River, for example, 50 km downstream from Flix, ~50 m^3 s^{-1} are diverted to two irrigation channels. This significant reduction in river discharge expectedly results in a reduction of the recuperation distance. Hence, X_{st} should be considered as an indicator of the intensity of the alteration that can be used by managers to decide on the appropriate spatial scale on which to conduct more detailed modeling studies or monitoring. Additionally, X_{st} contains more information than $T_{0m} - T_{st,m}$, since it is also an indicator of the resiliency of the river to thermal alteration.

[35] While water temperature in unaltered reaches of streams and rivers tends to reach steady state temperature, in major rivers it seems probable that for some reaches and periods, water temperature would not reach the steady state under certain circumstances (high discharge, thermal pollution, etc.). *Caissie et al.* [2005] found better agreement between their equilibrium temperature model and measurements for a stream than for a river, and performance was worse when snowmelt occurred. *Arrúe and Alberto* [1986] also found that snowmelt-caused high flows induced a clear decrease in water temperature in a middle course location in the Ebro River. In fact, even if the actual distances for thermal recuperation are probably shorter than X_{st} in the lower Ebro River because of the water abstraction, the distance necessary to attain steady state would often still be hundreds of kilometers. Thus, if such circumstances preventing the attainment of a steady state are not taken into account, estimations of the magnitude of alterations or of secondary heat exchanges (shading, groundwater, etc.) based on steady state temperatures may be biased. However, the objectives of our study did not include investigating water temperature in natural conditions or whether water temperature was in steady state at the entrance to the system of reservoirs.

[36] Still, our study has demonstrated another possible source of error when using the equilibrium temperature T_e in climate change studies, such as those by *Mohseni et al.* [1999], *Koch and Vögele* [2009], and *Rübbelke and Vögele* [2011], or as a base reference to assess alteration intensity or to detect additional sources/sinks of heat [e.g., *Bogan et al.*, 2004]. As shown in section 5.4 and Table 3, there are significant differences of ~1°C between equilibrium temperature T_e and mean daily steady state temperature $T_{st,m}$, arising from the method used to calculate each one. In both cases the net sum of heat fluxes over the day is zero. The difference is that for T_e a constant value is assumed and daily mean values of meteorological variables are used, whereas T_{st} is a time-varying variable calculated using time-varying meteorological data. Since the calculation of $T_{st,m}$ follows more closely the riverine thermal processes, it should be preferred over T_e in this kind of study to avoid bias.

7. Conclusions

[37] The heat balance of the river has been shown to be modified in response to thermal alterations. In order of importance of the heat flux modification, the processes altered by water temperature changes in the lower Ebro River are: evaporation, sensible heat exchange, and emission of long-wave radiation. Evaporation can have a limiting role in the capacity of the river to lose heat after a thermal discharge.

[38] Water temperature alterations depend greatly on discharge and its variability. In the first place, the rate of discharge influences the distance necessary for water temperature to attain the steady state independent of the type of alteration (regulation or thermal effluent): The higher the discharge, the longer the distance. Second, the intensity of the alteration for thermal discharges depends on discharge by means of the dilution effect. In this case, sharp variations of flow can cause sharp variations in water temperatures and increase water temperature variability. The variability of flow rate can also induce irregularity in the pattern of nodes and antinodes of water temperature range downstream from reservoirs.

[39] For an accurate estimation of the intensity of the alterations produced by infrastructures, actual water temperatures should be compared to steady state or mean daily steady state temperatures. Water temperatures downstream from the system of reservoirs of Mequinensa, Riba-roja, and Flix are higher than steady state temperature in the fall and lower during the rest of the year due to the alterations. The nuclear power plant increases water temperature throughout the year. Thus, in the fall the nuclear power plant effect is added to the previous warming effect due to the system of reservoirs and results in a further increase of the alteration. During the rest of the year, the nuclear power plant resists the reservoirs' cooling effect, resulting in a reduction of $T_{0m} - T_{st,m}$ and of X_{st}. The recuperation distance depends on the discharge, magnitude of the alteration, and climatological factors, and can embrace hundreds of kilometers in the lower Ebro River.

[40] **Acknowledgments.** The authors would like to thank ENDESA, the Ascó Nuclear Plant, CH Flix, and the Miravet City Council for their help and for providing a place to install the measurement stations. Part of the data presented here was the result of projects CGL2004-05503-C02-01/02/HID

and GL2008-06377-C02-01/02 funded by the Programa de Recursos Hídricos del Plan Nacional de Investigación y Desarrollo. One of the authors has been supported by an FPI grant from the Programa de Recursos Hídricos del Plan Nacional de Investigación y Desarrollo and the European Social Fund.

References

Arrúe, J. L., and F. Alberto (1986), El régimen térmico de las aguas superficiales de la Cuenca del Ebro, *An. Estac. Exp. Aula Dei*, *18*(1–2), 31–50.

Aubinet, M. (1994), Longwave sky radiation parameterizations, *Sol. Energy*, *53*(2), 147–154, doi:10.1016/0038-092X(94)90475-8.

Bogan, T., O. Mohseni, and H. G. Stefan (2003), Stream temperature-equilibrium temperature relationships, *Water Resour. Res.*, *39*(9), 1245, doi:10.1029/2003WR002034.

Bogan, T., H. G. Stefan, and O. Mohseni (2004), Imprints of secondary heat sources on the stream temperature/equilibrium temperature relationship, *Water Resour. Res.*, *40*, W12510, doi:10.1029/2003WR002733.

Bonacci, O., D. Trninić, and T. Roje-Bonacci (2008), Analysis of the water temperature regime of the Danube and its tributaries in Croatia, *Hydrol. Processes*, *22*, 1014–1021, doi:10.1002/hyp.6975.

Caissie, D., M. G. Satish, and N. El-Jabi (2005), Predicting river water temperatures using the equilibrium temperature concept with application on Miramichi River catchments (New Brunswick, Canada), *Hydrol. Processes*, *19*, 2137–2159, doi:10.1002/hyp.5684.

Campbell, J. W., and T. Aarup (1989), Photosynthetically available radiation at high latitudes, *Limnol. Oceanogr.*, *34*(8), 1490–1499.

Champion, P. D., and C. C. Tanner (2000), Seasonality of macrophytes and interaction with flow in a New Zealand lowland stream, *Hydrobiologia*, *441*(1–3), 1–12.

Cunge, J. A. (1969), On the subject of a flood propagation computation method (Muskingum Method), *J. Hydraul. Res.*, *7*(2), 205–230, doi:10.1080/00221686909500264.

de Doncker, L., P. Troch, R. Verhoeven, K. Bal, N. Desmet, and P. Meire (2009), Relation between resistance characteristics due to aquatic weed growth and the hydraulic capacity of the River Aa, *River Res. Appl.*, *25*(10), 1287–1303, doi:10.1002/rra.1240.

Dolz, J., J. Puertas, and E. Herrero (1994), Water temperature alteration downstream from a reservoir. The Ebro river case (Spain), *Commission International de Grands Barrages*, *69*, 211–225.

Edinger, J. E., D. W. Duttweiler, and J. C. Geyer (1968), The response of water temperatures to meteorological conditions, *Water Resour. Res.*, *4*(5), 1137–1143, doi:10.1029/WR004i005p01137.

Edinger, J. E., D. K. Brady, and J. C. Geyer (1974), Heat exchange and transport in the environment, *report 14, publication 74-049-00-3*, Electric Research Institute, Palo Alto, Calif.

Frutiger, A. (2004), Ecological impacts of hydroelectric power production on the River Ticino. Part 1: Thermal effects, *Arch. Hydrobiol.*, *159*(1), 43–56, doi:10.1127/0003-9136/2004/0159-0057.

Gu, R., S. McCutcheon, and C.-J. Chen (1999), Development of weather-dependent flow requirements for river temperature control, *Environ. Manage.*, *24*(4), 529–540, doi:10.1007/s002679900252.

Hamblin, P. F., and S. O. McAdam (2003), Impoundment effects on the thermal regimes of Kootenay Lake, the Arrow Lakes Reservoir and Upper Columbia River, *Hydrobiologia*, *504*(1–3), 3–19, doi:10.1023/B:HYDR.0000008503.75784.ee.

Henderson-Sellers, B. (1986), Calculating the surface energy balance for lake and reservoir modelling: A review, *Rev. Geophys.*, *24*(3), 625–649, doi:10.1029/RG024i003p00625.

Janssen, P. H. M., and P. S. C. Heuberger (1995), Calibration of process oriented models, *Ecol. Model.*, *83*(1–2), 55–66, doi:10.1016/0304-3800(95)00084-9.

Khangaonkar, T., and Z. Yang (2008), Dynamic response of stream temperatures to boundary and inflow perturbation due to reservoir operations, *River Res. Appl.*, *24*, 420–433, doi:10.1002/rra.1088.

Koch, H., and S. Vögele (2009), Dynamic modelling of water demand, water availability and adaptation strategies for power plants to global change, *Ecol. Econ.*, *68*, 2031–2039, doi:10.1016/j.ecolecon.2009.02.015.

Lessard, J. L., and D. B. Hayes (2003), Effects of elevated water temperature on fish and macroinvertebrate communities below small dams, *River Res. Appl.*, *19*(7), 721–732, doi:10.1002/rra.713.

Limnos (1997), *Estudi dels Efectes de l'Abocament Tèrmic de la Central Nuclear d'Ascó sobre les Comunitats Biològiques*, Junta de Sanejament, Barcelona, Spain.

Lowney, C. L. (2000), Stream temperature variation in regulated rivers: Evidence for a spatial pattern in daily minimum and maximum magnitudes, *Water Resour. Res.*, *36*(10), 2947–2955, doi:10.1029/2000WR900142.

Meier, W., C. Bonjour, A. Wüest, and P. Reichert (2003), Modeling the effect of water diversion on the temperature of mountain streams, *J. Environ. Eng.*, *129*(8), 755–764, doi:10.1061/(ASCE)0733-9372(2003)129:8(755).

Mohseni, O., and H. G. Stefan (1999), Stream temperature/air temperature relationship: A physical interpretation, *J. Hydrol.*, *218*(3–4), 128–141, doi:10.1016/S0022-1694(99)00034-7.

Mohseni, O., T. R. Erickson, and H. G. Stefan (1999), Sensitivity of stream temperatures in the United States to air temperatures projected under global warming scenario, *Water Resour. Res.*, *35*, 3723–3733, doi:10.1029/1999WR900193.

Polehn, R. A., and W. C. Kinsel (1997), Transient temperature solution for stream flow from a controlled temperature source, *Water Resour. Res.*, *33*(1), 261–265, doi:10.1029/96WR03016.

Ponce, V. M. (1989), *Engineering Hydrology. Principles and Practices*, 640 pp., Prentice Hall, Upper Saddle River, N. J.

Prats, J., R. Val, J. Armengol, and J. Dolz (2007), A methodological approach to the reconstruction of the 1949-2000 water temperature series in the Ebro River at Escatrón, *Limnetica*, *26*(2), 293–306.

Prats, J., J. Dolz, and J. Armengol (2009), Variabilidad temporal en el comportamiento hidráulico del curso inferior del río Ebro, *Ing. Agua*, *16*(4), 259–272.

Prats, J., R. Val, J. Armengol, and J. Dolz (2010), Temporal variability in the thermal regime of the lower Ebro River (Spain) and alteration due to anthropogenic factors, *J. Hydrol.*, *387*(1–2), 105–118, doi:10.1016/j.jhydrol.2010.04.002.

Preece, R. M., and H. A. Jones (2002), The effect of Keepit Dam on the temperature regime of the Namoi River, Australia, *River Res. Appl.*, *18*, 397–414, doi:10.1002/rra.686.

Pujol, L., and J. A. Sánchez-Cabeza (1999), Determination of longitudinal dispersion coefficient and velocity of the Ebro River waters (Northeast Spain) using tritium as a radiotracer, *J. Environ. Radioactiv.*, *45*(1), 39–57, doi:10.1016/S0265-931X(98)00075-7.

Pujol, L., and J. A. Sánchez-Cabeza (2000), Use of tritium to predict soluble pollutants transport in Ebro River waters (Spain), *Environ. Pollut.*, *108*(2), 257–269, doi:10.1016/S0269-7491(99)00185-2.

Raddum, G. G., A. Fjellheim, and G. Velle (2008), Increased growth and distribution of *Ephemerella aurivillii* (Ephemeroptera) after hydropower regulation of the Aurland catchment in Western Norway, *River Res. Appl.*, *24*(5), 688–697, doi:10.1002/rra.1142.

Rübbelke, D., and S. Vögele (2011), Impacts of climate change on European critical infrastructures: The case of the power sector, *Environ. Sci. Policy*, *14*, 53–63, doi:10.1016/j.envsci.2010.10.007.

Sabater, F., J. Armengol, and S. Sabater (1989), Measuring discontinuities in the Ter River, *Reg. Rivers Res. Manage.*, *3*, 133–142, doi:10.1002/rrr.3450030113.

Schaefli, B., and H. V. Gupta (2007), Do Nash values have value?, *Hydrol. Processes*, *21*(15), 2071–2080, doi:10.1002/hyp.6825.

Sill, B. L. (1983), Free and forced convection effects on evaporation, *J. Hydraul. Eng.*, *109*(9), 1216–1231, doi:10.1061/(ASCE)0733-9429(1983)109:9(1216).

Stanford, J. A., and J. V. Ward (2001), Revisiting the serial discontinuity concept, *Reg. Rivers Res. Manage.*, *17*(4–5), 303–310, doi:10.1002/rrr.659.

Steel, E. A., and I. A. Lange (2007), Using wavelet analysis to detect changes in water temperature regimes at multiple scales: Effects of multi-purpose dams in the Willamette River basin, *River Res. Appl.*, *23*, 351–359, doi:10.1002/rra.985.

Tang, H. S., and T. R. Keen (2009), Analytical solutions for open-channel temperature response to unsteady thermal discharge and boundary heating, *J. Hydraul. Eng.*, *135*(4), 327–332, doi:10.1061/(ASCE)0733-9429(2009)135:4(327).

Val, R. (2003), Incidencia de los embalses en el comportamiento térmico del río Ebro. Caso del sistema de embalses de Mequinenza-Ribarroja-Flix en el río Ebro, PhD thesis, Dept. of Hydraul., Marit. and Environ, Eng., Tech. Univ. of Catalonia, Barcelona, Spain.

Wåhlin, A. K., and H. L. Johnson (2009), The salinity, heat, and buoyancy budgets of a coastal current in a marginal sea, *J. Phys. Oceanogr.*, *39*, 2562–2580, doi:10.1175/2009JPO4090.1.

Ward, J. V., and J. A. Stanford (1983), The serial discontinuity concept of lotic ecosystems, in *Dynamics of Lotic Ecosystems*, edited by T. D.

Fontaine and S. M. Bartell, pp. 29–42, Ann Arbor Scientific Publishers, Ann Arbor, Mich.

Ward, J. V., and J. A. Stanford (1995), The serial discontinuity concept: Extending the model to floodplain rivers, *Reg. Rivers Res. Manage.*, *10*(2–4), 159–168, doi:10.1002/rrr.3450100211.

Webb, B. W., and F. Nobilis (1994), Water temperature behaviour in the River Danube during the twentieth century, *Hydrobiol.*, *291*, 105–113, doi:10.1007/BF00044439.

Webb, B. W., and D. E. Walling (1993), Temporal variability in the impact of river regulation on thermal regime and some biological implications, *Freshwater Biol.*, *29*(1), 167–182, doi:10.1111/j.1365-2427.1993.tb00752.x.

Webb, B. W., and Y. Zhang (1997), Spatial and seasonal variability in the components of the river heat budget, *Hydrol. Processes*, *11*(1), 79–101, doi:10.1002/(SICI)1099-1085(199701)11:1<79::AID-HYP404>3.0.CO;2-N.

Webb, B. W., and Y. Zhang (2004), Intra-annual variability in the non-advective heat energy budget of Devon streams and rivers, *Hydrol. Processes*, *18*(11), 2117–2146, doi:10.1002/hyp.1463.

Wilcock, R. J., P. D. Champion, J. W. Nagels, and G. F. Croker (1999), The influence of aquatic macrophytes on the hydraulic and physic-chemical properties of a New Zealand lowland stream, *Hydrobiologia*, *416*(1), 203–214.

Willmott, C. J., and K. Matsuura (2005), Advantages of the mean absolute error (MAE) over the root mean square error (RMSE) in assessing model performance, *Clim. Res.*, *30*(1), 79–82, doi:10.3354/cr030079.

World Wildlife Federation (WWF) (2009), *The Potential Impact of Climate Change on Stream Water Temperatures*, 26 pp., Frankfurt am Main, Germany.

Zolezzi, G., A. Siviglia, M. Toffolon, and B. Maiolini (2010), Thermopeaking in Alpine streams: event characterization and time scales, *Ecohydrology*, *4*(4), 477–612. doi:10.1002/eco.132.

J. Armengol, Department of Ecology, Faculty of Biology, University of Barcelona, Avda. Diagonal 645, 08028 Barcelona, Spain.

J. Dolz and J. Prats, Department of Hydraulic, Maritime and Environmental Engineering, Technical University of Catalonia, C. Jordi Girona 1-3, Building D1, Office D208, 08034 Barcelona, Spain. (jordi.prats-rodriguez@upc.edu)

R. Val, PUMAGUA, Universidad Nacional Autónoma de México, Torre de Ingeniería, 5° piso, ala norte, cubículo 3, Av. Universidad 3000, Ciudad Universitaria, 04510, México.